The Journal *of* Immunology

Microheterogeneity in the Kinetics and Sex-Specific Response to Type I IFN ⊘

Shani T. Gal-Oz; ... et. al

Related Content

A Method for Preparing Monospecific Antisera to C1 Esterase (C1s): Microheterogeneity of Purified C1s

J Immunol (July,1970)

Biochemical and biologic characterization of murine monocyte chemoattractant protein-1. Identification of two functional domains.

J Immunol (April,1994)

Endogenous pyrogens made by rabbit peritoneal exudate cells are identical with lymphocyte-activating factors made by rabbit alveolar macrophages.

J Immunol (May,1980)

Microheterogeneity in the Kinetics and Sex-Specific Response to Type I IFN

Shani T. Gal-Oz,* Alev Baysoy,[†] Brinda Vijaykumar,[†] Sara Mostafavi,[‡] Christophe Benoist,[†] Tal Shay,* and the Immunological Genome Project[1]

The response to type I IFNs involves the rapid induction of prototypical IFN signature genes (ISGs). It is not known whether the tightly controlled ISG expression observed at the cell population level correctly represents the coherent responses of individual cells or whether it masks some heterogeneity in gene modules and/or responding cells. We performed a time-resolved single-cell analysis of the first 3 h after in vivo IFN stimulation in macrophages and CD4^{+} T and B lymphocytes from mice. All ISGs were generally induced in concert, with no clear cluster of faster- or slower-responding ISGs. Response kinetics differed between cell types: mostly homogeneous for macrophages, but with far more kinetic diversity among B and T lymphocytes, which included a distinct subset of nonresponsive cells. Velocity analysis confirmed the differences between macrophages in which the response progressed throughout the full 3 h, versus B and T lymphocytes in which it was rapidly curtailed by negative feedback and revealed differences in transcription rates between the lineages. In all cell types, female cells responded faster than their male counterparts. The ISG response thus seems to proceed as a homogeneous gene block, but with kinetics that vary between immune cell types and with sex differences that might underlie differential outcomes of viral infections. *The Journal of Immunology*, 2024, 213: 96–104.

Type I IFNs are primordial elements of immunologic defenses and key mediators in a variety of immunological processes. The main players in the type I IFN family are IFN-α and IFN-β (designated IFN-α/β), which can be produced by almost all of the cells in the body and are therefore involved in a wide range of processes (1). Although the main focus of IFN activity is antiviral protection downstream of innate receptors, its influence extends to adaptive responses and autoimmune pathways (1–4). In many cell types, engagement of IFN-α/β surface receptors by IFN-α/β induces the expression of several hundred IFN signature genes (ISGs) (1, 4–7) in a largely coordinated manner (8). Underlying this ISG induction is a complex regulatory network that associates feed-forward components (e.g., induction of Stat1 and Stat2 transducers) with negative feedback (USP18 or SOCS induction) (4, 7, 9). IFN signaling can be regulated through a variety of target proteins, for example, USP18 (encodes for the IFN-inducible cysteine protease Ubp43) targets IFNAR2, the suppressor of cytokine signaling (Socs1) targets TYK2, and IFN regulatory factor (IRF) Irf2 targets other IRFs (10). Whereas the heterogeneity in IFN production between single cells has been studied widely (11, 12), the heterogeneity in the response to IFN has mostly been shown at the cell population level. For example, ISG expression levels differ between cells of different types or cells of the same type from healthy people compared with people with rheumatoid arthritis or systemic lupus erythematosus (SLE) (13). The dependence of ISG score on cell type and response time has been shown in single

hematopoietic stem and progenitor cells (14), which are inherently very heterogeneous, and their stimulation by IFN affects differentiation. However, despite intensive studies charting this network and investigating the response to IFN and the transcriptional profile of ISGs in different cell populations, in both health and disease, it is not known whether the response to IFN is homogeneous in single cells of the same type, in terms of the rate and direction in transcriptional space. Such knowledge would provide a better understanding of the regulation and coordination of the changes that occur within tissues and within individuals after exposure to IFN and could potentially reveal a subcellular population taking part in the response to IFN and possibly acting differently in males and females and affecting sexual dimorphism.

Alongside the heterogeneity of the cell response within an individual, additional factors can contribute to different responses between individuals. One of the factors currently thought to influence the IFN response is sexual dimorphism. In the immune system, sexual dimorphism may be manifested by a higher risk for autoimmunity but a better response to pathogens in females (15). For example, 9 of 10 patients with the autoimmune disease SLE are females (16). In many infectious diseases, including COVID-19, males tend to suffer severe or fatal disease more frequently (17), but greater severity of some other viral diseases has been reported in females (18). In addition to the differences in the frequency and severity of diseases, sex-specific differences in disease manifestations, comorbidities, and drug metabolism have also been reported (19). The metabolic pathways

---

*Department of Life Sciences, Ben-Gurion University of the Negev, Beer-Sheva, Israel; [†]Department of Immunology, Blavatnik Institute, Harvard Medical School, Boston, MA; and [‡]Paul G. Allen School of Computer Science and Engineering, University of Washington, Seattle, WA

[1]See members at http://www.immgen.org/.

ORCIDs: 0000-0001-7775-2006 (S.T.G.-O.); 0000-0001-5526-5848 (A.B.); 0000-0003-0755-1350 (T.S.).

underlying these differences are yet to be identified, but it has been suggested that IFN response pathways contribute both to the superior response of females to pathogens and to their higher risk of autoimmunity (18). Examples of the enhanced activity of IFN pathways in females (humans and mice) include higher expression of ISGs in the T cells of patients with HIV (20), in the neutrophils of healthy humans (21), and in the monocytes of patients with chronic low-grade inflammation (22), and also in naive and IFN-stimulated mouse macrophages (23). Despite the research that has been conducted, and the growing body of evidence of sexual dimorphism in a variety of immune-mediated conditions, the mechanisms underlying sexual dimorphism in the response to IFN remain to be elucidated.

Single-cell transcriptomics provide the framework to explore the heterogeneity of the cells responding to IFN and to reveal how tightly the transcriptional changes described at the cell population level are coordinated at the single-cell level. Additionally, because the immune response is a gradual and not a discrete process, studies at single-cell resolution have the power to identify transient stages that might be masked in the averaged signal studied in cell populations. Indeed, several studies have explored the transcriptional responses to IFN at the single-cell resolution in health (21), in viral infections (24–26) (specifically COVID-19 [9, 27–32]), in SLE (33, 34), and in intestinal epithelial cells (35). Nonetheless, none of these studies provides a broad view of the developing response to IFN in different (sorted) immune cell types of the same individual simultaneously, and, similarly, most did not test for differences between sexes.

Our previous RNA sequencing (RNA-seq) studies analyzed the response in vivo to IFN in several immune cell types and the underlying regulatory network in mice (7, 23), but the averaging of responses inherent in bulk profiling left several open questions unanswered: 1) Do all individual cells within a given cell type actually respond to IFN stimulation, and, if so, do they respond at the same rate? 2) Does the integrated population-level response of a given cell type represent the response of all cells, or do different cells activate different modules of ISGs that together comprise the prototypic response? 3) Do the different ISG responses between sexes represent different kinetics or amplitudes? To answer these questions and to reveal cell-specific kinetics and regulatory modes, we conducted a single-cell RNA-seq (scRNA-seq) study of three IFN-stimulated cell types that present qualitatively different responses at the cell population level (7). The three cell types were chosen as representatives of the major lineages of immunocytes, namely, from the myeloid lineage, peritoneal cavity macrophages, and from the lymphoid lineage, splenic CD4$^+$ T cells and B cells.

Materials and Methods

Mice and IFN treatment

C57BL/6J 5-wk-old male and female mice (The Jackson Laboratory) were injected i.v. with IFN-α or 100 μl of PBS. After 1 h, two mice of each sex (one from the IFN group and one from the PBS group) were sacrificed. After 2 and 3 h, one mouse of each sex in the IFN group was sacrificed (Supplemental Table I). Data were collected in two independent experiments (datasets A and B) for a total of eight male and seven female mice (Supplemental Table I). Both datasets were generated with the protocol described above, with the following differences: 1) the mice in dataset A were littermates; 2) the dosage of IFN-α in dataset A was calculated relative to the mouse weight (0.27 μl/g), whereas for dataset B a uniform dosage (10 μl) was administered (Supplemental Table I); and 3) dataset B did not include a female mouse at 2 h. Animal experimentation was approved by the Harvard Medical School Institutional Animal Use and Care Committee (protocol IS00001257).

Cell preparation and sorting

From each mouse, CD4 T and B cells from the spleen and macrophages from the peritoneal cavity were double sorted (Supplemental Table I). The ImmGen SOP (https://www.immgen.org) for the 14-cell set preparation was followed for CD4 T cells, B cells, and macrophages. Peritoneal cavity lavages were harvested after euthanasia by i.p. injection and aspiration of 10 ml of FACS buffer (phenol red-free DMEM, 2% FBS, 0.1% azide, and 10 mM HEPES [pH 7.9]). Splenic tissue was homogenized thoroughly through a 100-μm filter and centrifuged, and erythrocytes were lysed in ACK lysing buffer (Lonza, 1 ml per spleen) for 3 min at 4°C, centrifuged, washed, and resuspended in FACS buffer. Hashtag oligonucleotides (HTOs) were used to distinguish between mice of different sexes, injection types, and time points (Supplemental Table I). Cells were stained and double sorted according to the standard ImmGen 14-cell set; the second sort was performed directly into a LoBind tube containing 5 μl of TCL buffer (Qiagen) with 1% (v/v) 2-ME. Immediately after the sort, cells were kept on ice for 5 min, spun down, and frozen on dry ice. Cells were then pooled and profiled by 10x Genomics 3′ scRNA-seq.

scRNA-seq analysis

Downstream analyses were performed independently on the two datasets. Reads were aligned to the mouse genome (mm10, GENCODE M25 release [GRCm38.p6], https://www.gencodegenes.org/mouse/release_M25.html) using CellRanger (10x Genomics) to obtain gene counts. The CITE-seq-Count package (36) was used to assign reads to HTOs. Gene and HTO counts were then analyzed using Seurat v4 package (37). The HTODemux function was used to assign HTOs to single cells to identify the studied time points after IFN injection (0, 1, 2, or 3 h) and the sex of the cell. For preliminary filtering, only genes that were expressed by at least 10 cells and cells that expressed between 200 and 5000 or 200 and 7000 genes (datasets A and B, respectively) and <5% mitochondrial genes were analyzed. Cells with two barcodes (doublets) or cells with no barcode (negative) were eliminated from the analysis. For more details about choice of filtering criteria, see Supplemental Note 1, section 2.

Data were normalized using NormalizeData and scaled using ScaleDate (scaling was performed on all genes) functions of Seurat, with default parameters. The FindVariableFeatures function was used to identify the 2000 most variable genes ("vst" method). Principal component (PC) analysis was performed using the RunPCA function (with the identified variable genes). Uniform manifold approximation and projection (UMAP) dimensionality reduction was calculated on the first 15 PCs using the RunUMAP function. To identify cell types, shared nearest neighbor and thereafter Louvain clustering were performed on the first 15 PCs using the FindNeighbors and FindClusters functions with a cluster resolution of 1.5.

Cell clusters were assigned to cell types according to the expression of known cell type marker genes: macrophages: *Icam2, Adgre1, Cd14*; CD4 T cells: *Trbc1, Trbc2, Cd4, Il7r*; and B cells: *Cd19, Ms4a1, Cd79a*. Cells that expressed the cell type–specific markers but also expressed proliferation markers (*Mki67, Top2a*), cells that expressed both B cell and T cell markers, and CD4 T cells that also expressed a regulatory T cell marker (*Foxp3*), NK markers (*Klrd1, Klrk1, Nkg7*), or CD8 T cell markers (*Cd8a, Cd8b1*), or cells that were not assigned to one of the three cell types were removed from the analysis. For more details see Supplemental Note 1, section 1. Those clusters were not used for analysis other than cell type assignment. After cell type assignment and filtering, 9,285 cells expressing 15,764 genes remained in the analysis in dataset A, and 6,195 cells expressing 16,527 genes remained in dataset B. Normalization, scaling, and dimensional reduction were performed again for the remaining cells as described above (using the first 10 PCs). For downstream analyses after cell type identification, the datasets were split (using subset function) by cell type. Within each cell type, a second filtering step was performed, keeping genes that were expressed by at least 10 cells. Only cells that expressed between 500 and 5000 genes (macrophages) or 200 and 3000 genes (B and CD4 T cells) in dataset A and between 1000 and 6000 genes (macrophages) or 750 and 4000 genes (B and CD4 T cells) in dataset B were included in the analysis. The 2000 most variable genes identified using the FindVariableFeatures function were used to calculate PCs. UMAP, shared nearest neighbor (on the 10 first PCs for B and CD4 T cells and the 15 first PCs for macrophages) and clustering (cluster resolution = 1) analyses were performed with the same functions as mentioned above. Small and distinct nontypical cell clusters were attributed to sorting imperfection (not belonging to the sorted populations of CD4 T cells, B cells, or macrophages) and therefore removed from analysis, and filtered data were then normalized and scaled again with same parameters as before. Differentially expressed genes (DEGs) were identified using the FindMarkers function from Seurat with default values and filtered for genes with an adjusted *p* value of <0.05.

The data were produced in two batches (datasets A and B) that correspond to two 10x runs, which were different in the number of reads per cell. Thus, instead of batch correction, datasets A and B were analyzed separately. Additionally, the same individual isogenic mice were used across the three studied cell types, not showing any significant and consistent interindividual variability that justifies a correction.

ISGs

ISGs were previously defined by Mostafavi et al. (7) as genes upregulated in at least 1 out of 11 studied cell types, with a >2-fold induction and a positive false discover rate <0.1 (975 genes). Of those ISGs, 134 genes that were significantly upregulated after IFN stimulation in the original study in the three cell types studied (macrophages, CD4 T cells, and B cells) were termed in this study core ISGs. To overcome sparsity and calculate an accurate cell-specific score, only the core ISGs that were expressed above zero in at least 200 cells (of each cell type) in the current study (dataset A) were included in the analysis as cell type expressed ISGs (111, 99, and 92 genes in macrophages, CD4 T cells, and B cells, respectively). To determine the level of the response to IFN in single cells, a "response state" score was defined for each cell as the average expression of the 90 shared ISGs between the three lists of cell type–expressed ISGs. The shared and cell type–expressed ISGs were defined based on dataset A (Supplemental Table II), and the same gene sets were used in dataset B. The results were robust to the selection of the ISGs (Supplemental Note 1, section 3). Comparisons between response state distributions were performed with the "compare_means" function from ggpubr R package (https://github.com/kassambara/ggpubr/), using a *t* test and the Holm method (38) (default) for multiple comparison corrections.

Velocity analysis

The velocyto command line tool (Python implementation) (39) was used to obtain counts of spliced and unspliced reads and to create a loom file. Reads that mapped to multiple loci or mapped to repetitive elements (derived from expression repeat annotation, as downloaded from UCSC, as described in the velocyto user guide) were discarded. The loom file was then analyzed using scVelo (40) with a generalized dynamical model. Metadata, cell filtering, and UMAP calculation were taken from the Seurat analyses described above. Only cells that passed filtering in the Seurat analysis (dataset A: 3292, 3118, and 2282 cells in macrophages, CD4 T cells, and B cells, respectively; dataset B: 1694, 2076, and 2272 cells in macrophages, CD4 T cells, and B cells, respectively) and highly variable genes with at least 20 counts for spliced and unspliced RNAs (dataset A: 1093, 714, and 683 genes in macrophages, CD4 T cells, and B cells, respectively; dataset B: 1653, 1029, and 970 genes in macrophages, CD4 T cells, and B cells, respectively) were retained for the velocity analysis. Normalization, modeling of transcriptional dynamics, and estimation of RNA velocities were performed using the "dynamical" mode and default parameters in scVelo (40). Single-cell velocities were projected onto the precomputed UMAP embedding from Seurat for visualization. The length of the velocity vectors (given by velocity_length parameter) were obtained from scVelo to describe the rate (or speed) of the transcriptional changes throughout the response to IFN.

Data availability

All scRNA-seq datasets generated in this manuscript (datasets A and B) have been deposited in the Gene Expression Omnibus under accession number GSE242117 (https://www.ncbi.nlm.nih.gov/geo/query/acc.cgi?acc= GSE242117).

Results

Single-cell resolution transcriptional map of early IFN response in three immune cell types

Young adult male and female C57BL/6J mice were injected i.v. with IFN-α or vehicle (control mice), and cells were harvested at three time points, that is, 1, 2, or 3 h later. Cells were "hash-tagged" with DNA-barcoded Abs (41) before purification by flow cytometry; this methodology was applied to enable the joint processing and analysis of all time points, an important design approach that enables robust comparison of transitional intermediates. Two independent experiments were performed, with one dataset (dataset A) serving as the primary dataset and the other (dataset B) providing replication (see Supplemental Figs. 1, 3–5). After scRNA-seq and data processing, cells belonging to each population were filtered for singlets and the usual quality criteria (excluding NKT cells, regulatory T cells, and proliferating cells) to yield 3292 macrophages, 3118 CD4 T cells, and 2282 B cells in dataset A.

Cell type–specific response to IFN

The cells of each of the three cell types formed an elongated blob having distinct "start" and "end" regions following the application of the UMAP (Fig. 1A, Supplemental Fig. 1A). UMAP projection is based on dimensionality reduction (PC analysis) and allows the visualization of the multidimensional gene expression data in two dimensions, where each point represents a cell and neighboring cells are transcriptionally similar. The cell types clearly differ in the kinetics of their response to IFN. Macrophages from consecutive time points occupied neighboring but distinct regions of the UMAP, suggesting that all macrophages responded quasi-synchronously and that their response was coherent and continuous over time. For CD4 T cells, the progression of the response was more heterogeneous, although almost all of the cells eventually progressed to the end region. The cells of 1 h after IFN exposure were widely scattered throughout the UMAP space and almost equally distributed between the regions occupied by untreated control cells (45%) and those occupied by most CD4 T cells of 3 h after IFN exposure (55%). At the 3 h time point, the CD4 T cells included a minor, but distinct, proportion (8%) of cells that appeared to be refractory to the action of IFN (in contrast to macrophages). The ~300 regulatory T cells that were set aside showed the same spread as the other CD4 T cells (data not shown). B cells also displayed a heterogeneous progression; this progression was somewhat faster than that for CD4 T cells, as 82% of the 1 h B cells occupied the end region, with fewer "laggards" than for the CD4 T cells. Here again, a small proportion (5%) of nonresponder B cells was present at the 3 h time point. The above-described differences in the heterogeneity of progression were formalized by computing a "response state," based on the expression of 90 ISGs induced in macrophages and CD4 T and B cells in both Mostafavi et al. (7) and in the current data. In all three cell types, the distributions of the response states at each time point were in keeping with the UMAP projection, which was computed using an independently selected set of the most variable genes, and together the response states and the UMAP projection indicated that the ISGs are representatives of the overall process (Fig. 1B, 1C, Supplemental Fig. 1B, 1C). In addition, we observed a significant decline in the response state between 2 h and 3 h only in the B cells (*t* test, Holm adjusted $p = 5.2 \times 10^{-14}$; Fig. 1B, 1C, right). This decline was also observed in dataset B but did not reach a significant level (Supplemental Fig. 1B, 1C, right). Thus, in answer to our first question, by 3 h the vast majority of cells did take part in the ISG response, with the exception of a small minority of B and T lymphocytes, but with different kinetics for the different cell types.

Negative regulation contributes to cell type–specific kinetics

It is possible that a faster negative regulation in B cells compared with macrophages and CD4 T cells is responsible to the decline in response between 2 and 3 h observed in B cells. To test this, we compared the gene expression levels of three prominent negative regulators of IFN response, Usp18, Irf2, and Soc1, throughout the time points. The expression pattern of all three negative regulators is consistent to that of the response state across stimulation time points (Supplemental Fig. 2). Usp18 expression level increases in macrophages at least up to 3 h, but peaks at 2 h in CD4 T and B cells (Supplemental Fig. 2A). Socs1 expression level peaks at 2 h in macrophages and CD4 T cells, and at 1 h in B cells (Supplemental Fig. 2B). Irf2 gene expression peaks at 2 h in B cells, but is still upregulated between 2 and 3 h in macrophages and CD4 T cells (Supplemental Fig. 2C). All three representative negative regulators of the IFN response, which act through different target proteins, display an earlier peak in B cells, suggesting that the different kinetics of the transcriptional response between the cell types is tightly regulated by different kinetics of negative regulators.
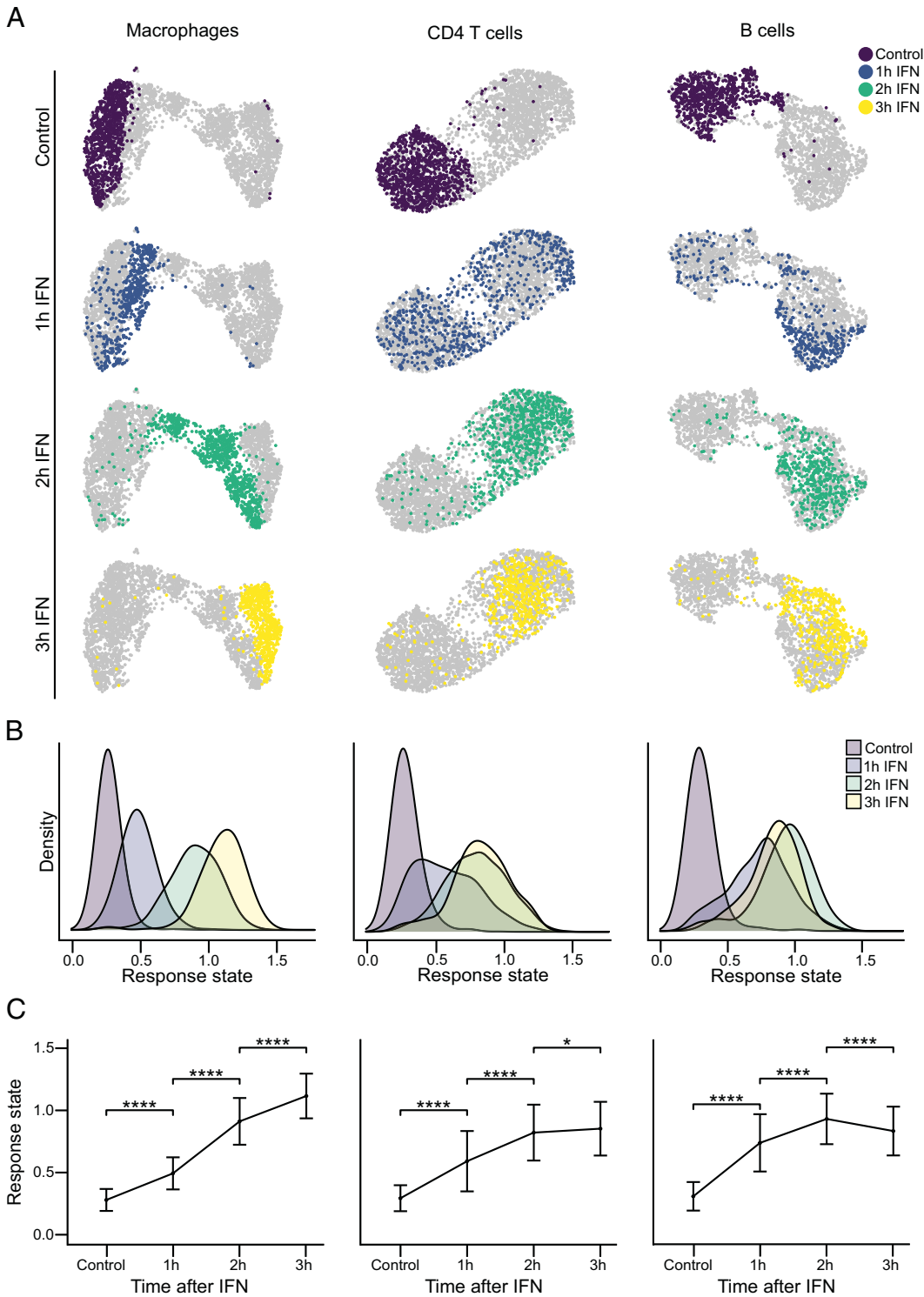
FIGURE 1. Cell type–specific dynamics of the response to IFN. (**A**) UMAP plot calculated for each cell type separately. For each stimulation time point (top to bottom, 0, 1, 2, and 3 h after stimulation), only cells of the relevant time point are highlighted in color, and the other cells are shown in gray. (**B**) Response state distribution of the cells at each time point. (**C**) Average response state per cell at each time point. For (A)–(C) shown from left to right: macrophages (3292 cells), CD4 T cells (3118 cells), and B cells (2282 cells). $*p \leq 0.05$, $****p \leq 0.0001$ for different distributions between time points by a two-sided t test (Holm adjusted).

Single trajectory of response and correlation between response state and rate

The above results provided snapshots of the response state of each cell at the time of harvest. To estimate the rate at which each cell evolved with respect to ISG expression and the trajectory followed, we performed RNA velocity analysis, which exploits the ratio of immature (partially spliced) to mature transcripts as a proxy for the rate of transcription of selected genes and to infer cells transcriptional trajectories (39, 40). For each cell type, when all time points were treated together, a main trajectory led from control to 1 h and then 2 and 3 h (Fig. 2A, Supplemental Fig. 3A); such a trajectory was also observed when velocity vectors were calculated separately
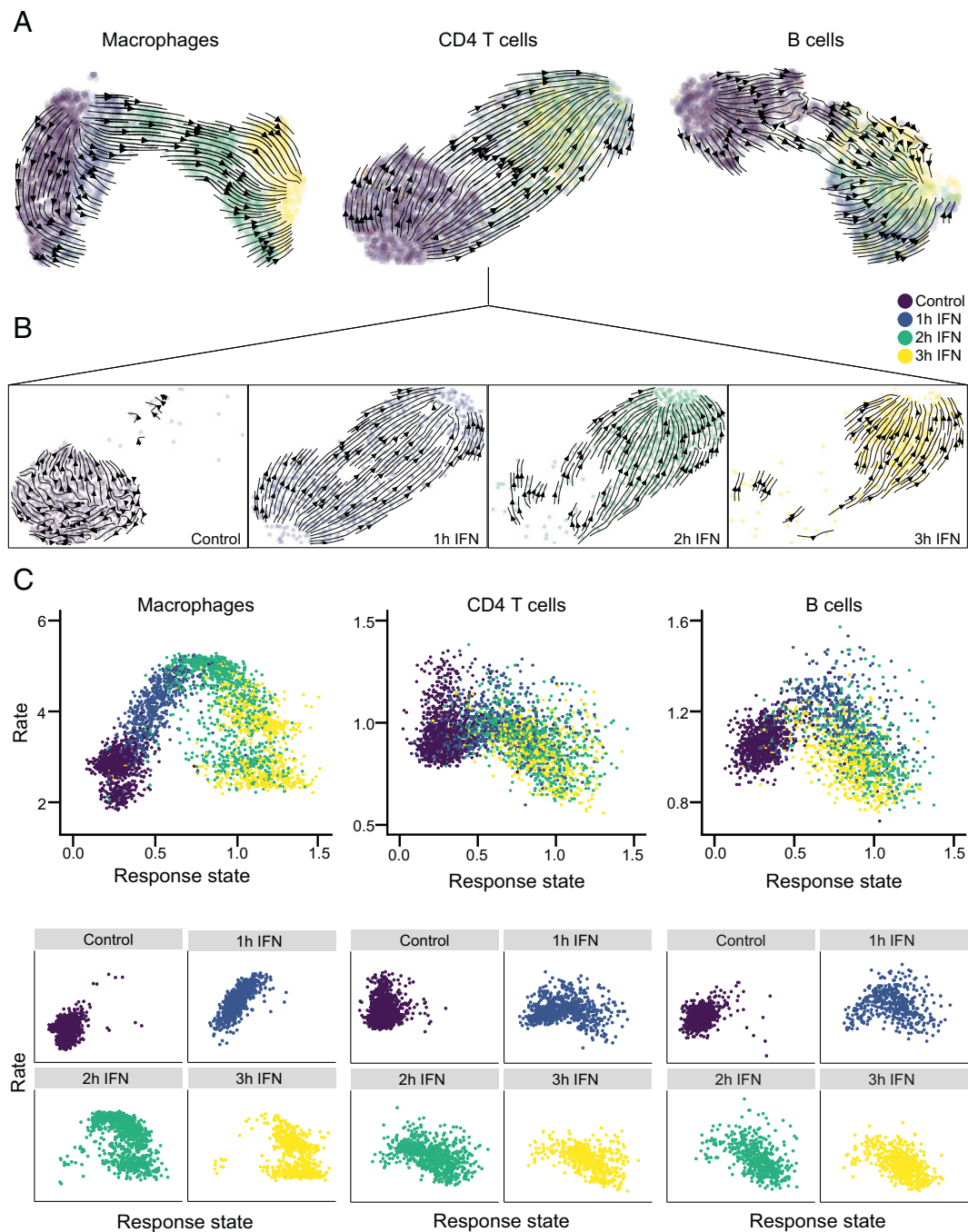
FIGURE 2. All cells of the same type move along the same transcriptional trajectory after IFN stimulation. (**A**) Velocities derived from the dynamical model of scVelo (visualized as streamlines) projected on the UMAP space for macrophages, CD4 T cells, and B cells (left to right). Cells are colored by their IFN stimulation time point. (**B**) Velocities of CD4 T cells calculated separately for each time point. From left to right: control and 1, 2, and 3 h after IFN stimulation. (**C**) Rate of response (given by velocity vector length) compared with response state in macrophages, CD4 T cells, and B cells (left to right), shown for all cells (top) and per time point (bottom).

for each time point (Fig. 2B, Supplemental Fig. 3B); that is, at times 1, 2, and 3 h, all stimulated cells pointed in the same direction. We then asked how these rates of progression related to the integrated response state: Would high response states in some cells reflect a higher rate, or would they instead show lower rates, indicating that negative feedback was coming into play, as suggested by the upregulation of negative regulators? Conversely, would apparent laggards show correspondingly slow rates of response, or would they "attempt to catch up"? Plotting the state versus rate estimates proved illuminating in that it revealed a strong difference between cell types

(Fig. 2C, Supplemental Fig. 3C). For macrophages, a linear relationship between state and rate at 1 h subsequently slowed down at 2 and 3 h, indicating that the rate of induction was the main factor changing throughout the response. For T and B lymphocytes, the early correlation was largely missing; instead, there was a negative correlation between response state and rate (which was strongest at 2 h). These results, together with the expression pattern of representative negative regulators (Supplemental Fig. 2), suggest that the limitation of ISG responses by negative feedback (4) comes into play very rapidly in lymphocytes, but only later in macrophages.

We noted a separation into two groups in macrophages, which was clearest at baseline and at 3 h, where some of the macrophages had an intrinsically higher rate. Differential gene expression analysis at baseline and at 3 h showed that the same genes differed between fast and slow rate macrophages at both time points (Supplemental Table III). The differentially expressed genes included Myc targets and cell cycle genes, which suggests that the subgrouping of macrophages corresponds to inherently different states, not specifically related to IFN responses.

Homogeneity of the IFN response transcriptional modules

To address our second question of whether all ISGs are similarly induced in all cells, we searched for the existence of cell clusters in which particular ISG modules were differentially expressed, with focus on ISGs that were induced above a minimal threshold in each cell type (Supplemental Table II). We observed a generally coherent expression of ISGs in all cells of the same type at the same time point, except for the quantitative variation in the integrated response states described above (Fig. 3, Supplemental Fig. 4; the refractory CD4 T and B cells were particularly noticeable as darker columns in the heatmaps). The level of gene–gene correlation varied between some groups of ISGs. However, the groups of the more highly correlated genes were composed of the more highly expressed genes, and no groups of cells with different expression patterns were observed, thus suggesting that this gene

clustering is not due to different expression patterns but is affected by the sparsity in lower expression levels. Thus, no distinct patterns of ISG induction were identified as influencing cell clusters. To test whether there is a cell type–specific heterogeneity arising from genes that are not included in the shared list of ISGs used above, we also evaluated the heterogeneity of DEGs between control and 3 h after stimulation. Even though some DEGs were previously defined as ISGs (7), no additional heterogeneity in gene expression patterns was identified (Supplemental Note 1, section 4). DEGs were enriched for the expected Gene Ontology terms such as "defense response to virus" and "innate immunity."

The coherent expression change of the ISGs suggests a shared regulation. Out of the 90 shared ISGs used in the current study (Supplemental Table II), 79 appear in the list of genes bound by Stat2 in B cells induced by IFN (7), hinting at direct regulation by the canonical ISGF3 complex.

Sexual dimorphism in the response to IFN

Finally, we sought to test whether the single-cell resolution would provide a better understanding of the sexual dimorphism in the response to IFN (21, 23). In our previous study involving 11 immune cell types, macrophages showed the largest differential expression between sexes, and the genes that were overexpressed in resting or IFN-stimulated female macrophages relative to male macrophages were highly enriched for the IFN pathway (23). Our scRNA-seq
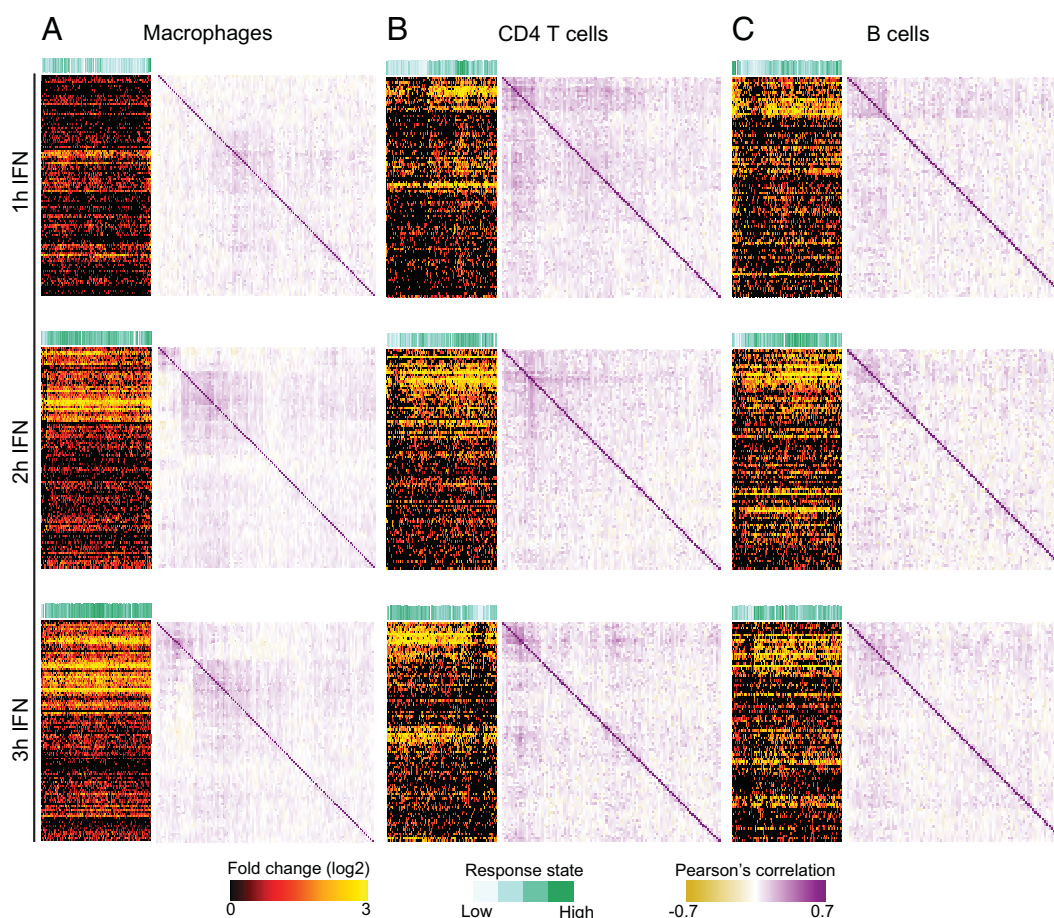
FIGURE 3. Response of ISGs is coherent among single cells. (**A**) Macrophages, (**B**) CD4 T cells, and (**C**) B cells at 1, 2, or 3 h after IFN stimulation. Expression heatmap (left) and Pearson correlation coefficient matrix (right) of the ISGs in female cells of each cell type are shown. Cells (columns in the expression heatmap) and ISGs (rows in the expression heatmap and rows and columns in the the correlation matrix) are sorted by clustering within each cell type and time point. White-green bars above expression heatmaps indicate response state. For each cell type, only the ISGs that were expressed in >200 cells were included: macrophages (111 ISGs), CD4 T cells (99 ISGs), and B cells (92 ISGs).

datasets in the current study included both male and female mice (with the exception that a technical failure resulted in no macrophages for male cells at the 3 h time point). Here again, macrophages showed the greatest sexual dimorphism, as demonstrated by the distinct UMAP regions occupied by male and female cells (Fig. 4A, Supplemental Fig. 5A). The sex differences were reflected in 210 DEGs between sexes in macrophages before IFN stimulation, and 389 DEGs at one or more time points after IFN stimulation (Supplemental Table IV). In accordance with the previously identified female upregulated DEGs in macrophages (23), higher response states were observed in female macrophages at all compared time points and also at intermediate time points in female CD4 T and B cells relative to their male counterparts ($p < 10^{-5}$, Fig. 4B, Supplemental Fig. 5B). DEGs lists were enriched for IFN response–associated genes, but no other functional enrichment term was significant. Thus, the difference between the sexes in terms of the response to IFN seemed to be cell type–dependent and to be manifested primarily in the rate of

the response, that is, female cells responded faster to IFN in all of the cell types tested.

Discussion

Type I IFNs are key mediators in a variety of immune processes, by inducing expression of a set of ISGs (1, 5–7). In addition to the antiviral and proinflammatory effects of type I IFNs, they are also involved in the pathology of autoimmune diseases and hyperinflammation (1–3, 31). To maintain a balanced immune response and limit the level of inflammation, the response to type I IFN is tightly regulated at multiple levels, including by some of the ISGs (9). Although ISGs have been extensively studied in health and disease, they were mainly characterized at the cell population level, and regardless of sex (7, 14). Hence, there is not much known about how these responses distribute among individual cells and between males and females.

This study describes the response of individual immune cells from male and female mice to IFN and provides clear answers to
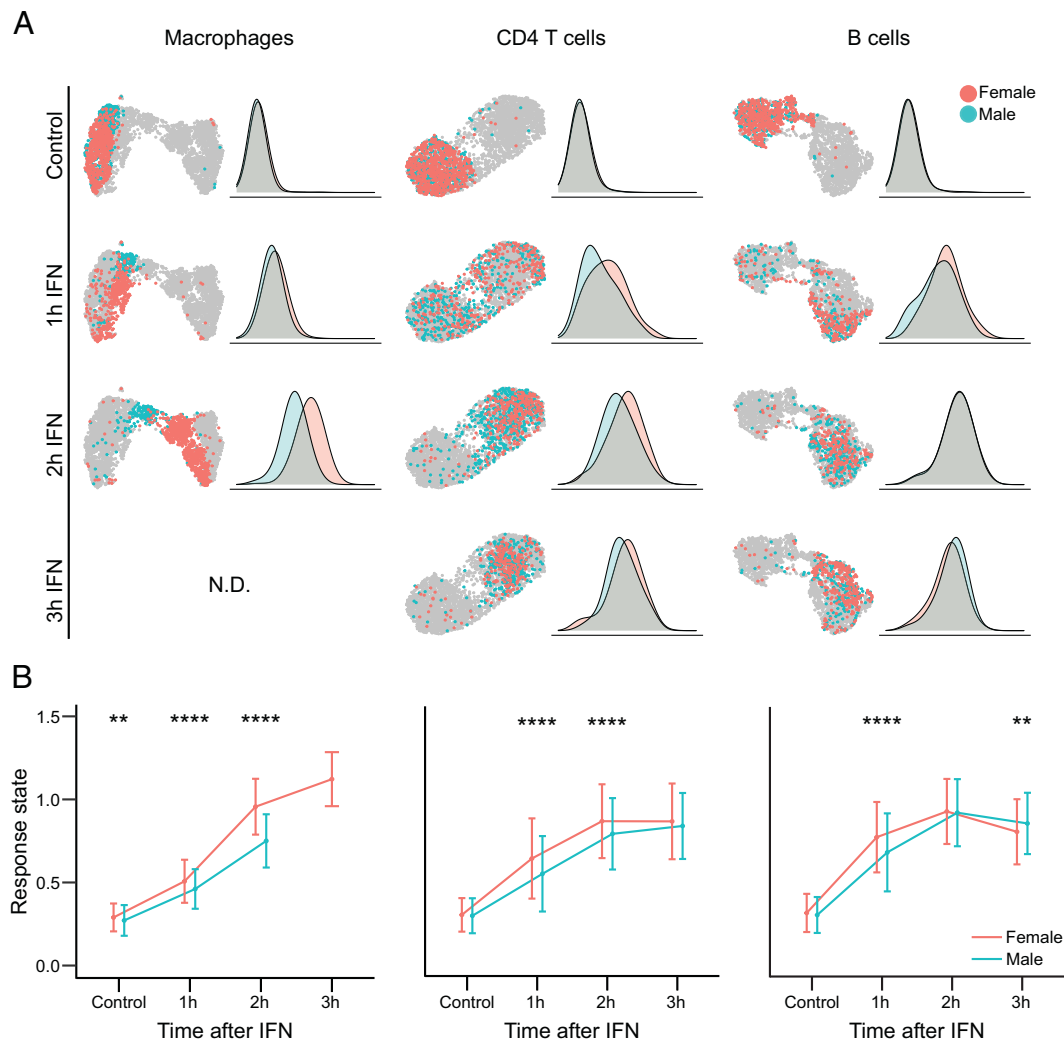

FIGURE 4. The rate of the transcriptional response of ISGs to IFN differs between sexes. (**A**) UMAP visualization (left) and its corresponding response state distribution (right) separated by time points and ordered top down from control to 1, 2, and 3 h for each cell type (columns, left to right): macrophages, CD4 T cells, and B cells. In macrophages, 3 h data were removed from the comparison due to an insufficient number of male cells for comparison purposes. (**B**) Average response state per cell at each time point for males (light blue) and females (pink) in macrophages (left), CD4 T cells (center), and B cells (right). **$p \leq 0.01$, ****$p \leq 0.0001$ for different distributions between the sexes (within each time point) by a two-sided t test (Holm adjusted).

two main questions formulated at the outset of the study. ISGs did indeed behave as a coregulated block, induced largely in concert in all cells, and there was no evidence of heterogeneity in the response of the induced gene modules or in the cells that induced them. All cells of the same type appeared to follow a single trajectory along transcriptional space. Distinct heterogeneity was, however, uncovered in terms of kinetics, particularly for CD4 T and B cells, with some cells reaching the maximal response state at 1 h, whereas other cells only partially responded, or not at all. We also identified minor, but distinct, subsets of CD4 T and B cells, which did not respond to IFN at any time point. Mechanistically, it may be speculated that these subsets comprise cells that reside in a shielded environment not reached by the injected IFN (although the i.v. injection route is expected to facilitate wide distribution of IFN-α, which is a small protein) or that the IFN signaling pathway is disconnected in some cells. From a functional standpoint, the missing antiviral state in the IFN-refractory cells might prove to be a liability in terms of the response to viral infection, but it might also lead to altered TCR responses, given the known cross-talk between TCR and IFN signaling (9, 42, 43).

The single-cell parsing also uncovered different dynamics between the three cell types, which were taken from the same animals after in vivo IFN stimulation. Macrophages showed the steadiest increase in the response state up to 3 h. These observations are consistent with reports in mice that monocytes express the highest ISG levels at baseline and in response to IFN stimulation compared with other cell types, including PBMCs (44) and bone marrow and spleen cells (45). The response in CD4 T and B cells rapidly showed signs of negative feedback, with a striking state/rate anticorrelation already evident at 1 h. ISG expression in B cells even appeared to "head back" at 3 h, in accordance with our prior kinetic analyses (7). Thus, extrapolating from the current set of cell types, the response to IFN appears to be less constricted in innate immunocytes than in adaptive immunocytes.

It is becoming increasingly evident that sex is an important factor in immune responses (15, 18, 19). Congruent with previous reports of higher expression of ISGs in females following immune stimulation (20, 21, 23), which was interpreted as a stronger response, the current study shows that the response is faster in female cells in all cell types. This difference in response rates can possibly contribute to the faster clearance of infections in females. However, in the peak points of the response of CD4 T cells (3 h) and B cells (2 h), there is no significant difference between male and female cells, suggesting that the amplitude of the peak response is the same in both sexes. Because immune responses, in particular those to viruses, are ultimately sensitive to small variations in the initial steps of activation (in essence a chaotic process), it may be speculated that sex differences at the onset of ISG induction ultimately have an important impact on antiviral resistance.

In summary, our results serve to deepen the understanding of the IFN response that was previously described in cell populations, in terms of response heterogeneity, kinetics, and sexual dimorphism. The distinction between stronger and faster in the early immune response to IFN is crucial for the efforts to incorporate sex effect into medical treatment, for example in determining sex-specific drug administration protocols and dosage (46). These findings will thus contribute to the study of IFN-mediated conditions and point the way to possible exploitation of the IFN pathway in biological and medical research.

Acknowledgments

Disclosures

References

1. McNab, F., K. Mayer-Barber, A. Sher, A. Wack, and A. O'Garra. 2015. Type I interferons in infectious disease. *Nat. Rev. Immunol.* 15: 87–103.
2. Banchereau, J., and V. Pascual. 2006. Type I interferon in systemic lupus erythematosus and other autoimmune diseases. *Immunity* 25: 383–392.
3. Wu, J., and Z. J. Chen. 2014. Innate immune sensing and signaling of cytosolic nucleic acids. *Annu. Rev. Immunol.* 32: 461–488.
4. Ivashkiv, L. B., and L. T. Donlin. 2014. Regulation of type I interferon responses. *Nat. Rev. Immunol.* 14: 36–49.
5. Schneider, W. M., M. D. Chevillotte, and C. M. Rice. 2014. Interferon-stimulated genes: a complex web of host defenses. *Annu. Rev. Immunol.* 32: 513–545.
6. Schoggins, J. W., S. J. Wilson, M. Panis, M. Y. Murphy, C. T. Jones, P. Bieniasz, and C. M. Rice. 2011. A diverse range of gene products are effectors of the type I interferon antiviral response. *Nature* 472: 481–485.
7. Mostafavi, S., H. Yoshida, D. Moodley, H. LeBoité, K. Rothamel, T. Raj, C. J. Ye, N. Chevrier, S. Zhang, T. Feng, et al.; Immunological Genome Project Consortium. 2016. Parsing the interferon transcriptional network and its disease associations. *Cell* 164: 564–578.
8. Zanin, N., C. Viaris de Lesegno, C. Lamaze, and C. M. Blouin. 2020. Interferon receptor trafficking and signaling: journey to the cross roads. *Front. Immunol.* 11: 615603.
9. Sumida, T. S., S. Dulberg, J. C. Schupp, M. R. Lincoln, H. A. Stillwell, P. Axisa, M. Comi, A. Unterman, N. Kaminski, A. Madi, et al. 2022. Type I interferon transcriptional network regulates expression of coinhibitory receptors in human T cells. *Nat. Immunol.* 23: 632–642.
10. Arimoto, K., S. Miyauchi, S. A. Stoner, J. Fan, and D. Zhang. 2018. Negative regulation of type I IFN signaling. *J. Leukoc. Biol.* 103: 1099–1116.
11. Wimmers, F., N. Subedi, N. van Buuringen, D. Heister, J. Vivié, I. Beeren-Reinieren, R. Woestenenk, H. Dolstra, A. Piruska, J. F. M. Jacobs, et al. 2018. Single-cell analysis reveals that stochasticity and paracrine signaling control interferon-alpha production by plasmacytoid dendritic cells. *Nat. Commun.* 9: 3317.
12. Van Eyndhoven, L. C., E. Chouri, N. Subedi, and J. Tel. 2021. Phenotypical diversification of early IFNα-producing human plasmacytoid dendritic cells using droplet-based microfluidics. *Front. Immunol.* 12: 672729.
13. El-Sherbiny, Y. M., A. Psarras, M. Y. Md Yusof, E. M. A. Hensor, R. Tooze, G. Doody, A. A. A. Mohamed, D. McGonagle, M. Wittmann, P. Emery, and E. M. Vital. 2018. A novel two-score system for interferon status segregates autoimmune diseases and correlates with clinical features. *Sci. Rep.* 8: 14846.
14. Bouman, B. J., Y. Demerdash, S. Sood, F. Grünschläger, F. Pilz, A. R. Itani, A. Kuck, V. Marot-Lassauzaie, S. Haas, L. Haghverdi, and M. A. Essers. 2024. Single-cell time series analysis reveals the dynamics of HSPC response to inflammation. *Life Sci. Alliance* 7: e202302309.
15. Klein, S. L., and K. L. Flanagan. 2016. Sex differences in immune responses. *Nat. Rev. Immunol.* 16: 626–638.
16. Beeson, P. B. 1994. Age and sex associations of 40 autoimmune diseases. *Am. J. Med.* 96: 457–462.
17. Scully, E. P., J. Haverfield, R. L. Ursin, C. Tannenbaum, and S. L. Klein. 2020. Considering how biological sex impacts immune responses and COVID-19 outcomes. *Nat. Rev. Immunol.* 20: 442–447.
18. Vom Steeg, L. G., and S. L. Klein. 2016. SeXX matters in infectious disease pathogenesis. *PLoS Pathog.* 12: e1005374.
19. Gal-Oz, S. T., and T. Shay. 2022. Immune sexual dimorphism: connecting the dots. *Physiology (Bethesda)* 37: 55–68.
20. Chang, J. J., M. Woods, R. J. Lindsay, E. H. Doyle, M. Griesbeck, E. S. Chan, G. K. Robbins, R. J. Bosch, and M. Altfeld. 2013. Higher expression of several interferon-stimulated genes in HIV-1–infected females after adjusting for the level of viral replication. *J. Infect. Dis.* 208: 830–838.
21. Gupta, S., S. Nakabo, L. P. Blanco, L. J. O'Neil, G. Wigerblad, R. R. Goel, P. Mistry, K. Jiang, C. Carmona-Rivera, D. W. Chan, et al. 2020. Sex differences in neutrophil biology modulate response to type I interferons and immunometabolism. *Proc. Natl. Acad. Sci. USA* 117: 16481–16491.
22. So, J., A. K. Tai, A. H. Lichtenstein, D. Wu, and S. Lamon-Fava. 2021. Sexual dimorphism of monocyte transcriptome in individuals with chronic low-grade inflammation. *Biol. Sex. Differ.* 12: 43.
23. Gal-Oz, S. T., B. Maier, H. Yoshida, K. Seddu, N. Elbaz, C. Czysz, O. Zuk, B. E. Stranger, H. Ner-Gaon, and T. Shay. 2019. ImmGen report: sexual dimorphism in the immune system transcriptome. *Nat. Commun.* 10: 4295.
24. Bomidi, C., M. Robertson, C. Coarfa, M. K. Estes, and S. E. Blutt. 2021. Single-cell sequencing of rotavirus-infected intestinal epithelium reveals cell-type specific epithelial repair and tuft cell infection. *Proc. Natl. Acad. Sci. USA* 118: e2112814118.
25. Li, H., X. Li, S. Lv, X. Peng, N. Cui, T. Yang, Z. Yang, C. Yuan, Y. Yuan, J. Yao, et al. 2021. Single-cell landscape of peripheral immune responses to fatal SFTS. *Cell Rep.* 37: 110039.
26. Lebratti, T., Y. S. Lim, A. Cofie, P. Andhey, X. Jiang, J. Scott, M. R. Fabbrizi, A. N. Ozantürk, C. Pham, R. Clemens, et al. 2021. A sustained type I IFN-neutrophil-IL-18 axis drives pathology during mucosal viral infection. *Elife* 10: e65762.
27. Hatton, C. F., R. A. Botting, M. E. Dueñas, I. J. Haq, B. Verdon, B. J. Thompson, J. S. Spegarova, F. Gothe, E. Stephenson, A. I. Gardner, et al. 2021. Delayed induction of type I and III interferons mediates nasal epithelial cell permissiveness to SARS-CoV-2. *Nat. Commun.* 12: 7092.

28. Sungnak, W., N. Huang, C. Bécavin, M. Berg, R. Queen, M. Litvinukova, C. Talavera-López, H. Maatz, D. Reichart, F. Sampaziotis, et al.; HCA Lung Biological Network. 2020. SARS-CoV-2 entry factors are highly expressed in nasal epithelial cells together with innate immune genes. *Nat. Med.* 26: 681–687.

29. Krämer, B., R. Knoll, L. Bonaguro, M. ToVinh, J. Raabe, R. Astaburuaga-García, J. Schulte-Schrepping, K. M. Kaiser, G. J. Rieke, J. Bischoff, et al. Deutsche COVID-19 OMICS Initiative (DeCOI). 2021. Early IFN-α signatures and persistent dysfunction are distinguishing features of NK cells in severe COVID-19. *Immunity* 54: 2650–2669.e14.

30. Schuurman, A. R., T. D. Reijnders, A. Saris, I. Ramirez Moral, M. Schinkel, J. de Brabander, C. van Linge, L. Vermeulen, B. P. Scicluna, W. J. Wiersinga, et al. 2021. Integrated single-cell analysis unveils diverging immune features of COVID-19, influenza, and other community-acquired pneumonia. *Elife* 10: e69661.

31. van der Wijst, M. G. P., S. E. Vazquez, G. C. Hartoularos, P. Bastard, T. Grant, R. Bueno, D. S. Lee, J. R. Greenland, Y. Sun, R. Perez, et al.; UCSF COMET consortium. 2021. Type I interferon autoantibodies are associated with systemic immune alterations in patients with COVID-19. *Sci. Transl. Med.* 13: eabh2624.

32. Jun, Y. C., S.-H. Kim, I. Jung, E.-C. Shin, S.-H. Park, S. H. Park, K. L. Heung, J. J. Su, J.-S. Kwon, M. Sa, et al. 2020. Immunophenotyping of COVID-19 and influenza highlights the role of type I interferons in development of severe COVID-19. *Sci. Immunol.* 5: eabd1554.

33. Deng, Y., Y. Zheng, D. Li, Q. Hong, M. Zhang, Q. Li, B. Fu, L. Wu, X. Wang, W. Shen, et al. 2021. Expression characteristics of interferon-stimulated genes and possible regulatory mechanisms in lupus patients using transcriptomics analyses. *EBioMedicine* 70: 103477.

34. Kotliarov, Y., R. Sparks, A. J. Martins, M. P. Mulè, Y. Lu, M. Goswami, L. Kardava, R. Banchereau, V. Pascual, A. Biancotto, et al. 2020. Broad immune activation underlies shared set point signatures for vaccine responsiveness in healthy individuals and disease activity in lupus patients. *Nat. Med.* 26: 618–629.

35. Triana, S., M. L. Stanifer, C. Metz-Zumaran, M. Shahraz, M. Mukenhirn, C. Kee, C. Serger, R. Koschny, D. Ordoñez-Rueda, M. Paulsen, et al. 2021. Single-cell transcriptomics reveals immune response of intestinal cell types to viral infection. *Mol. Syst. Biol,* 17: e9833.

36. Roelli, P, B. Bimber, B. Flynn, S. Revale, and G. Gui. 2019. Hoohm/CITE-seq-Count: 1.4.2. Available at: https://zenodo.org/doi/10.5281/zenodo.2585469.

37. Hao, Y., S. Hao, E. Andersen-Nissen, W. M. Mauck, S. Zheng, A. Butler, M. J. Lee, A. J. Wilk, C. Darby, M. Zager, et al. 2021. Integrated analysis of multimodal single-cell data. *Cell* 184: 3573–3587.e29.

38. Holm, S. 1979. A simple sequentially rejective multiple test procedure. *Scand. J. Stat.* 6: 65–70.

39. La Manno, G., R. Soldatov, A. Zeisel, E. Braun, H. Hochgerner, V. Petukhov, K. Lidschreiber, M. E. Kastriti, P. Lönnerberg, A. Furlan, et al. 2018. RNA velocity of single cells. *Nature* 560: 494–498.

40. Bergen, V., M. Lange, S. Peidli, F. A. Wolf, and F. J. Theis. 2020. Generalizing RNA velocity to transient cell states through dynamical modeling. *Nat. Biotechnol.* 38: 1408–1414.

41. Stoeckius, M., C. Hafemeister, W. Stephenson, P. Houck-Loomis, P. K. Chattopadhyay, H. Swerdlow, R. Satija, and P. Smibert. 2017. Simultaneous epitope and transcriptome measurement in single cells. *Nat. Methods* 14: 865–868.

42. Welsh, R. M., K. Bahl, H. D. Marshall, and S. L. Urban. 2012. Type 1 Interferons and antiviral CD8 T-cell responses. *PLoS Pathog.* 8: e1002352.

43. Marrack, P., J. Kappler, and T. Mitchell. 1999. Type I interferons keep activated T cells alive. *J. Exp. Med.* 189: 521–530.

44. Stifter, S. A., N. Bhattacharyya, A. J. Sawyer, T. A. Cootes, J. Stambas, S. E. Doyle, L. Feigenbaum, W. E. Paul, W. J. Britton, A. Sher, and C. G. Feng. 2019. Visualizing the selectivity and dynamics of interferon signaling in vivo. *Cell Rep.* 29: 3539–3550.e4.

45. Uccellini, M. B., and A. García-Sastre. 2018. ISRE-reporter mouse reveals high basal and induced type I IFN responses in inflammatory monocytes. *Cell Rep.* 25: 2784–2796.e3.

46. Tannenbaum, C., and D. Day, Matera Alliance. 2017. Age and sex in drug development and testing for adults. *Pharmacol. Res.* 121: 83–93.